

Research article

Three Dimensional Photoelastic Investigation for Analyzing Stress Concentration Factor in Isotropic Square Simply Supported Plate with Hole Subjected to Transverse Loading

Moon Banerjee^{1*}, Nitin Kumar Jain² and Shubhashis Sanyal²

¹*Department of Mechanical Engineering, Koneru Lakshmaiah Educational Foundation, Hyderabad, Telangana-500075, India*

²*Department of Mechanical Engineering, National Institute of Technology, Raipur, India*

Received: 20 May 2021, Revised: 21 November 2021, Accepted: 14 January 2022

DOI: 10.55003/cast.2022.05.22.010

Abstract

Keywords

three-dimensional photoelasticity;
finite element method;
stress freezing phenomenon;
stress concentration factor

In this paper, an experimental and numerical study was carried out to examine stress concentration fields near singularities, originating and propagating in accordance with different hole diameter to width ratios (D/A) in a square plate. Experimental three-dimensional photoelastic analyses were performed to predict the reaction of geometric conditions, loading and boundary condition on stress concentration factor (SCF) near the hole. During experimental analysis, stress was locked inside the plate by the use of stress freezing technique. Further evaluation of locked stress was performed with a polariscope, with the help of slices procured using the slicing method employed on stress frozen plate. The different fringes obtained from monochromatic and white light showed the variation of maximum intensity stresses which were further compared with the stress contours from the finite element model. Also, assessment was conducted with the finite element method to validate the results. Based on the results, percentage variation between experimental and analytical was evaluated and it was found that the variation was between 2 and 5%.

1. Introduction

The failure of mechanical components is often due to the presence of discontinuities like cracks, holes, or any notches within the component. This discontinuity directly or indirectly hampers the strength of the component. For the above reason, a designer should be acquainted with the propagation of stress and stress concentration factors near the irregularities. Three-dimensional

*Corresponding author: Tel.: (+91) 7999626421

E-mail: moonbanerjee@gmail.com

photoelasticity has been considered to be one of the most powerful approaches. The current work aims to determine the concentration of stress under vertical loading in relation to different boundary conditions.

There has been a lot of practical research work already performed on the analysis of stress and SCF in the field of three-dimensional photoelasticity. Ramakrishnan and Ramesh [1] developed different scanning methods for use in photoelasticity. In this work, the precision of the ordered fringes was improved by mapping the isometric fringe pattern into spatial resolution. Ramesh and Deshmukh [2] proposed the three fringe method for the photoelastic approach, which gave good results compared to conventional results. This was based on the complete analysis flexible seeding approach for solving problems. Patil *et al.* [3] used digital photoelasticity to evaluate tip fracture parameters using a linear least square approach method. Also, the ten step method was employed with AQGPU algorithm for determination of stress field equations. Assessment of results was further done by an analytical method. The results showed that the value of stress intensity factor for cracked tip solved for ten different parameters were in good agreement with photoelasticity and FEA. Perumal *et al.* [4] formed two generalized equations for thin plates with holes using extended FEM. The work emphasized on usage of equations that are helpful for solving both linear and nonlinear boundaries, thus reducing solution error in a significant percentage. Ramesh and Ramakrishnan [5] performed a comprehensive review on digital photoelasticity of glass. The work was focused on residual stress in glass, with an initial focus on its tensile character. Recent advances in digital photoelasticity are discussed in accordance with accurate determination of photoelastic constant. Surface stress in flat glass was determined by surface guided waves. Ajovalasit *et al.* [6] reviewed the RGB photoelasticity in depth. Their work was mainly concerned with taking images in white light photoelasticity, and a single image for the determination of relative retardation was proposed. Swain *et al.* [7] evaluated a new technique for RGB photoelasticity. In their paper, a reference table was made with the help of a synthetic bending experiment associated with computer program for RGB calibration. Shang *et al.* [8] studied a digital phase shifting method for the generation of isoclinic fringes. Enab [9] analyzed the behavior of functionally graded plates under biaxial loadings. In this paper, (SCF) was evaluated for a plate with an elliptical hole under different loading conditions. A set of parameters were taken as the minor and major axes of an elliptical hole, material properties, functionality, etc. Pandya and Parey [10] determined the stiffness of a cracked spur gear using optical methods. Both analytical and experimental methods were applied to evaluate the stiffness of the cracked pinion. Two-dimensional photoelasticity was used to assess the results. Kale and Ramesh [11] proposed a front scanning approach for three fringe photoelasticity. The proposed method established the incorporation of multiple seed points, which help with the proper management of scanning order for complex problems.

Many researchers [12-14] have worked in making prototype models using computer aided engineering associated with numerical and three dimensional photoelasticity. Two-dimensional photoelasticity with digital cameras has been used to procure the residual stresses under tensile forces.

According to the above literature review, we proposed to fill the gap in the research by doing further necessary work on three-dimensional photoelasticity. The objective of this research was to evaluate the SCF for a square plate with hole under transverse loading for two different boundary conditions. Moreover, complete procurement of stress and SCF near the discontinuity was performed by three-dimensional photoelasticity followed by validation with a finite element method. The results also differentiate the different isochromatic fringes obtained in both white and monochromatic light. To the best of the author's knowledge, no such performance assessment of simulation work by three-dimensional photoelasticity has been done.

2. Materials and Methods

A square plate of dimensions 0.2 m x 0.2 m and 0.01 m thickness was taken with a central circular hole of diameter (D), as shown in Figure 1. Transverse loading in the form of uniform distributed loading was applied over the plate with simply supported boundary conditions (Figure 2) at all edges. The diameter of the hole was varied from 0.02 to 0.06 m, respectively.

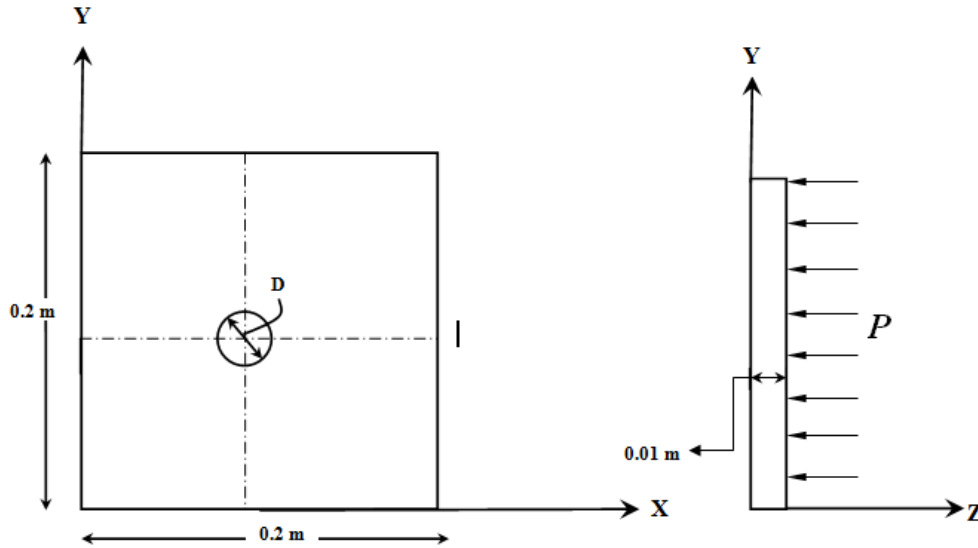


Figure 1. Dimensions of plate cast

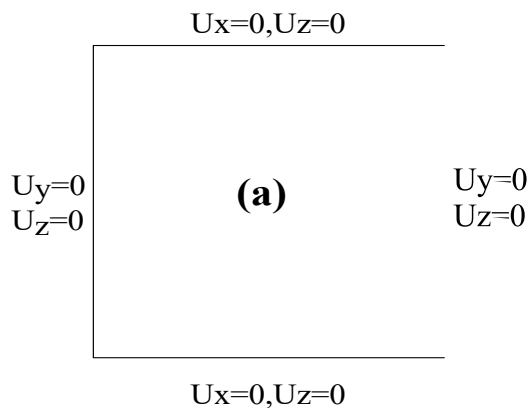


Figure 2. Simply supported boundary conditions

For each diameter of hole, two plates were cast and after stress freezing phenomenon, stress analysis was carried out. Square plate without holes (solid plates) was also used to evaluate the maximum stress.

Experimental photo elastic stress analysis was performed step by step as mentioned below. It involved casting of the model, stress freezing in an oven, slicing, sub-slicing and lastly optical analysis. The processes followed are explained further.

The procedures involved in making the specimen were preparation of the molds and mixing in proper proportion. Araldite CY-230 and ARADUR HY-951 were mixed in the proportion of 1:7. Numbering was done for all plates to avoid mixing the plates that had different hole diameters and boundary conditions. The numbering of model plates with different hole diameters and boundary conditions is tabulated in Table 1. Two sets of plates were made for each particular hole diameter and also two solid plates were made. The calibration disc was calibrated each time for material fringe values (f_{σ}) in every set of stress freezing cycles. Every set of stress freezing cycle consisted of one plate of a particular hole diameter and a calibration disc accommodated inside the stress freezing oven. This process was repeated for different set of plates with different hole diameters and for the solid plates.

Table 1. Sample numbering for different plates cast with circular holes

Boundary Condition	Diameter (mm)	Sample No
Simply Supported	20	1
		2
	50	3
		4
	60	5
		6
	Solid plate	7
		8

2.1 Stress freezing

Stress freezing is a process by which stresses are locked into the birefringent material using a thermal cycle involving heating above the glass transition temperature, as elaborated in Figure 3. Also, the stress freezing oven required for above process is shown in Figure 4.

The photoelastic model of the square plate and a calibration disc was placed in the stress freezing oven; and the temperature was raised slowly from room temperature to the stress freezing temperature of 70°C. The loading was done by applying a transverse load to the model at stress freezing temperature. This was continued for the next three hours during which time the model was soaking (second step). Next, the oven was cooled to room temperature at a slow rate in the order of 1 to 3°C per hour to avoid introduction of thermal stresses in the model (third state). The calibration specimen and model both underwent an identical stress freezing cycle in the oven.

The loading fixtures used inside the stress freezing oven for the above cycle is shown in the Figure 5. The first fixture shown in Figure 5 was used for evaluation of material fringe values and the second loading arrangement shows the arrangement of simply supported boundary condition. This stress freezing cycle was repeated for different samples.

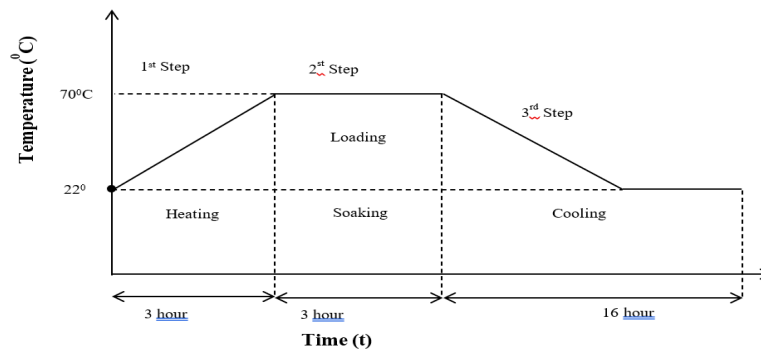


Figure 3. Stress freezing cycle



Figure 4. Stress freezing oven

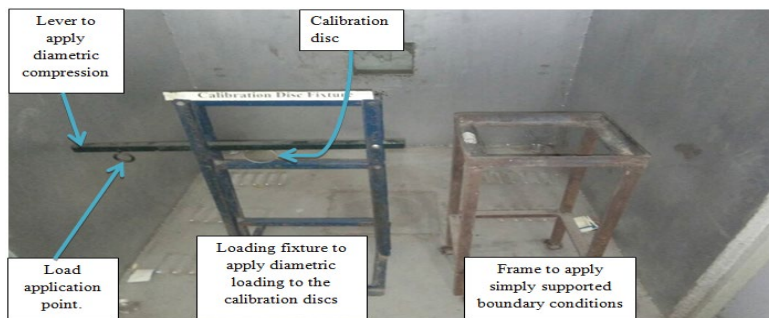


Figure 5. Loading fixture and boundary condition arrangement inside oven

2.2 Slicing and sub-slicing

The model is sliced to remove the planes of interest which can then be further examined individually to determine the state of stress existing in that particular plane of slice. Figure 6 shows the slicing plan employed in the model to remove and examine the slices, direction of view, final slices and slice thickness to be considered (h_y).

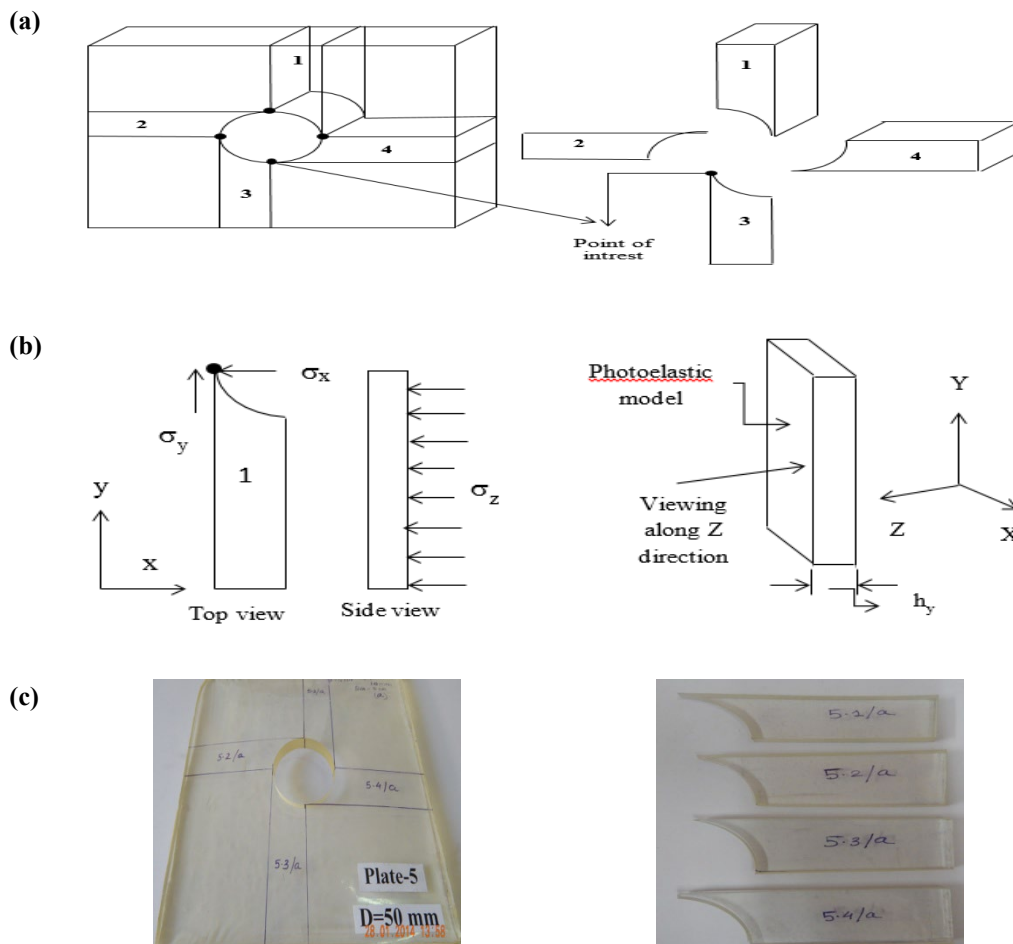


Figure 6. Slicing plan of the square plate with hole for boundary conditions: (a) Slicing plan, (b) Slicing analysis: - Direction of view in photoelastic bench, and (c) Final slices obtained

After cutting the slices as shown in Figure 7 as per the slicing plan, the surface of each slice was polished with the help of zero number polish paper. To ensure the accuracy of results, four slices from each plate were taken out. During the slicing operation, some of the slices were broken; collectively results were evaluated and discussed.

2.3 Sub-slicing plan for solid plate

Analysis of the solid plate (plate without hole) undergoing a similar stress freezing cycle for two different boundary conditions was performed differently in comparison to the plate with a hole. The sub-slicing plan for each solid plate and the thick dot showed the point of concern where the fringe counting is to be done as shown in Figure 8.

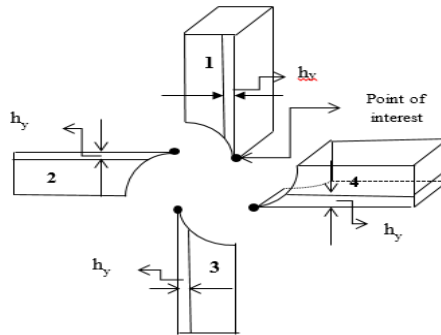


Figure 7. Slice thickness for plate model

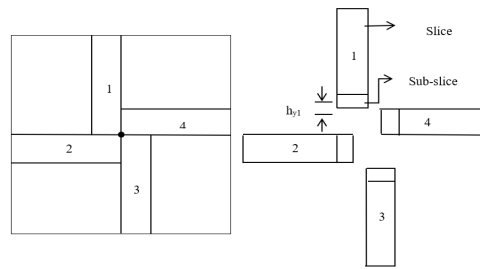


Figure 8. Sub-slicing plan for solid plate model

2.4 Nomenclature

A	area (m^2)	h_y	thickness of slice at the point of interest
D	diameter of the circular disk, (m)	N	Number of fringes
f_σ	fringe constant	P	load applied in circular disc (N)
g	gravity	x	distance from the center of the disc along the horizontal axis
h	slice thickness	$\sigma_x, \sigma_y, \sigma_z$	stress along X, Y, Z directions

3. Result and Discussion

Results were evaluated after the above-mentioned processes had been carried out sequentially. Thereafter, material fringe values were taken out by the circular disc for analysis. Since loading along the Z direction was known for both boundary conditions, stress along Z direction could thus be evaluated. Stress along the X direction was calculated by applying the stress optic law. It was calculated from the slices taken out from each plate with a hole and from the sub-slices of each solid plate. Using the above data σ_x with hole, σ_x without hole, SCF at the point of interest was determined. A circular polariscope with both light and dark field arrangement was utilized on the

photoelastic bench to evaluate fringe patterns near the point of concern. Digital pictures were taken in both white and monochromatic light in order to evaluate stress directions and for proper fringe counting. The results were evaluated by determining fringe patterns, and fringe orders results were evaluated. The mentioned steps taken are followed sequentially.

3.1 Calculation of material fringe value, (f_σ)

The material fringe value (f_σ) is defined as the number of fringes produced per unit load. The material fringe value is the property of the model material for a given wavelength and thickness of the model. The results of photoelastic stress analysis of a circular disc under diametric compression in the stress freezing oven are shown in Figure 9. Four different specimens were taken with diameters of 0.06 mm and 0.04, respectively. Based on the load applied on the circular disc, f_σ was evaluated for each specimen individually, and results are listed in Table 2. The material fringe value (f_σ) at critical temperature was determined using the equation 1 [2].

$$f_\sigma = \frac{8P(D^4 - 4D^2x^2)}{\pi DN(D^2 + 4x^2)^2} \quad (1)$$

At center of disc $x = 0$, thus we have material fringe value expression as:

$$f_\sigma = \frac{8P}{\pi DN} \quad (2)$$

The Table also clarifies the usage of the particular specimen for four different numbered plates.

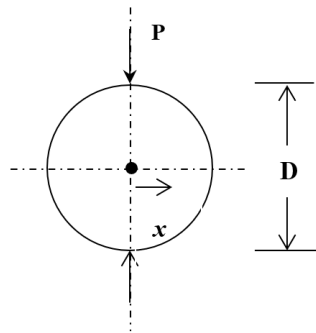


Figure 9. Calibration disc in compression

Table 2. Photoelastic results for the circular disc under stress freezing cycle

Specimen	Sample No.	D (m)	P (Kg)	P (Newton)	N	f_σ (N/m-fringe order)	Figure No.
1	1-2-9-10	0.06	2.0	19.62	7.5	111.0	8.4.1
2	3-4-11-12	0.06	1.6	15.69	4.5	147.9	
3	5-6-13-14	0.06	1.6	15.69	5.5	121.0	
4	7-8-15-16	0.04	4.0	39.24	22.5	111.0	

3.2 Experimental stress analysis

Experimental stress analysis of each square plate with a hole under transverse loading over the whole plate for simply supported boundary condition was performed after the above-mentioned process sequentially. Figure 10 shows the different calibration discs taken from different samples for the evaluation of fringe value f_{σ} . Equations 1 and 2 were used for evaluating the fringe value, by counting the number of fringes, diameter and other parameters. The images in Figure 10 were taken by the instrument shown in Figure 11.

A sand bag of mass 18 Kg was selected as the transverse load and was kept over the square plate for both boundary conditions. After a stress freezing cycle of the photoelastic model plate, slicing and sub-slicing was done in order to obtain stress values near the point of concern. Stress along X direction (σ_x) was evaluated, with known values of stress along Z direction σ_z , thus evaluated with the help of stress optic law. Also, material fringe value for each set of plates was obtained separately for each specimen as shown in Table 2 using the stress optic law.

3.3 Determination of stress along X-direction (σ_x)

By the application of stress optic law, the stress difference in a particular slice can be evaluated. For the square plate under symmetric boundary conditions,

$$\sigma_x = \sigma_y \quad (3)$$

From stress optic law, looking along y direction, we have [2]:

$$\sigma_x - \sigma_z = \frac{Nf_{\sigma}}{h_y} \quad (4)$$

The dimensions of square plate were taken to be 0.2 m x 0.2 m, but after loading, 0.005 m distance had to be left from each side of the square plate due to difference between the edges of the boundary condition fixture and the load application surface area. Thus, the new dimension of plate was taken as 0.195 m x 0.195 m. As a result, the stress along Z-direction for each plate is:

$$\sigma_z = \frac{F}{A} = \frac{mg}{A} = 4643.78 \text{ N/m}^2$$

$$\sigma_z = 18 \times 9.81 / 0.195 \times 0.195 = 4643.78 \text{ N/m}^2$$

Where, m= mass = 18 Kg

A= area in (m²) = 0.195 x 0.195

and g= gravity = 9.81 m/s²,

Also, for plate (b), σ_z is given by

$$\sigma_z = 3.5 \times 9.81 / 0.195 \times 0.195 = 902.95 \text{ N/m}^2$$

Rearranging equation (4):

$$\sigma_x = \sigma_z + \frac{Nf_{\sigma}}{h_y} \quad (5)$$

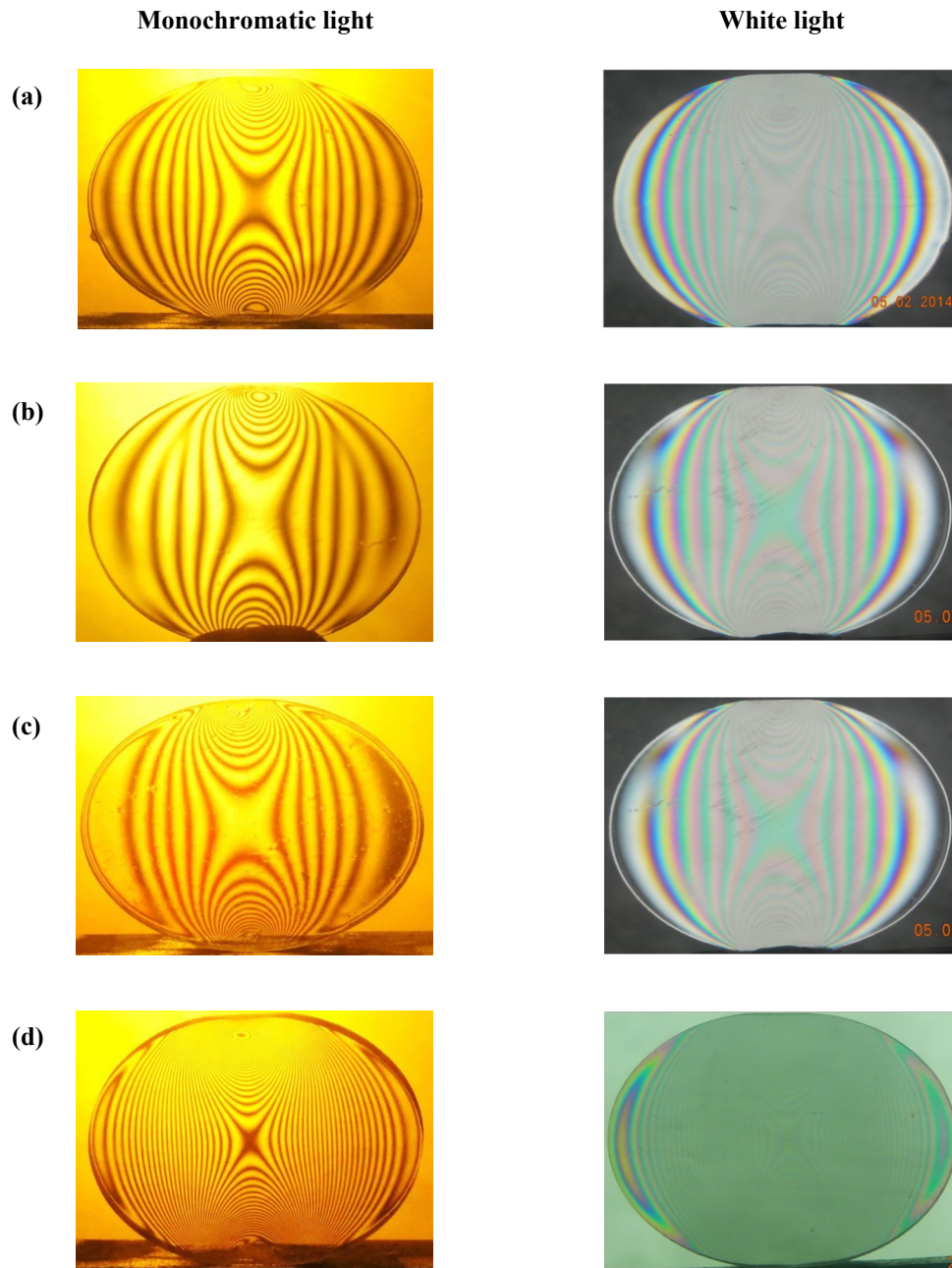


Figure 10. Isochromatic fringes in stress frozen calibration discs under monochromatic and white light for boundary conditions: (a) Specimen-1, (b) Specimen-2, (c) Specimen-3 and (d) Specimen-4

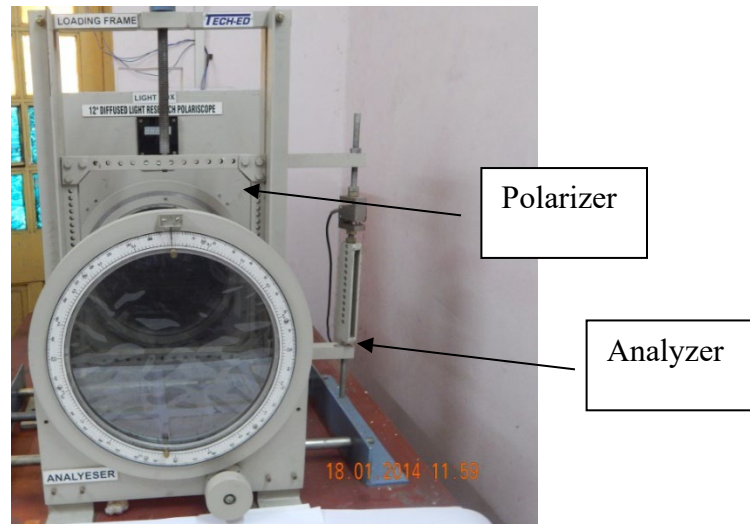


Figure 11. Photoelastic bench

Thus, for plate (a), putting the values in the equation:

$$\sigma_x = 4643.78 + \frac{N f_{\sigma}}{h_y} \quad (6)$$

Thus σ_x can be evaluated with the above equation for the known values of N , h_y and f_{σ} for each specimen separately. The number of fringes (N) was observed with the help of slices taken from plate with different hole diameters and sub-slices from the solid plates.

Analysis was carried out using both white and monochromatic light to confine the results in their stress directions and determine proper fringe contours. Since the boundary condition was symmetric, fringe contours obtained were symmetric in nature for all the stress frozen plate models. To obtain the fringes near the point of interest, the plates were sliced as per the slicing plan. After slicing, slices and sub-slices were analyzed in X and Z directions in order to obtain fringes near the point of interest. Marking and numbering of plates and slices were done as per the requirement. Slices and sub-slices were so machined so that no thermal stress accumulated while performing machining operation, which can clearly be seen in slice fringe patterns.

The photoelastic analysis for slices of plates 1 and 2 with hole diameter 0.02 m under circular polariscope and the dark field arrangement is shown in Table 3.

For each slice, pictures were taken from both X and Z directions. Slice 1.1/a refers to the first slice for plate number 1 and for boundary conditions. Similar patterns of numbering were followed for all slices and sub-slices of plates. All slices, when viewed along Z direction on the photoelastic bench provided confirmation of no thermal stress accumulation, as fringes did not get distorted in any of the slices, which is clearly observed. Fringe counting for slice 1.1/a was done by viewing along X direction, which showed the fringes near the point of concern marked as a thick dot in the zoomed-in view.

Moreover, under white light, stress direction based on different color fringe pattern was obtained and it was found that stress increased in an upward direction whereas with monochromatic light, fringe counting was done and the number of fringes obtained was 2. Similar observations were

Table 3. Fringe patterns for slices of samples 1 and 2 with hole diameter 0.02 m

Light	Slice No.	Z-Direction	X-Direction	Zoomed View	Fringe Direction and Counting
White	1.1				↑
	1.2				
	2.1				
	2.2				
Monochromatic	1.1				
	1.2				
	2.1				
	2.2				

carried out for remaining slices of plates 1 and 2 in order to ensure the accuracy by repeatability of results. Finally, the number of fringes obtained was 2.

The fringe patterns for slices in samples 3 and 4 under light field and circular polariscope arrangements are shown in Table 4. Moreover, under white light, stress direction based on different color fringe pattern was obtained and it was found that stress increased in an upward direction, whereas in the case of monochromatic light, fringe counting was performed and the number of fringes obtained was 1.5. The slice analysis of plates 5 and 6 under dark field and circular polariscope arrangement is shown in Table 5. Moreover, under white light, stress direction based on different color fringe pattern was obtained and it was found that stress increased in an upward direction, whereas using monochromatic light, fringe counting was performed and the number of fringes obtained was 2.

The sub-slice analysis of plates 7 and 8, which were the solid plates, under light field and circular field arrangement, is shown in Table 6. Moreover, under white light, stress direction based on different color fringe pattern was obtained and from monochromatic light, fringe counting was performed and the number of fringes obtained was 0.5.

Figure 12 (a) shows the the set of stress frozen plates just after the complete stress freezing cycle followed by further analysis under the photoelastic bench (b) forming isochromatic fringes under white and monochromatic light. Numbering and slice marking of the plates was performed in order to proceed with further in-depth analysis.

The % error in SCF calculated by following formula:

$$\% \text{ Error} = ((\text{SCF by photoelasticity} - \text{SCF by FEM}) / \text{SCF by FEM}) * 100 \quad (7)$$

The SCF evaluation of boundary condition is shown in Table 7. σ_x is calculated from equation 6 with the known values of f_σ , N and h_y calculated from the above Tables. Also, a comparison of experimental results with FEM results was done in order to check the accuracy of the results and it was found to be satisfactory. More than 50 plates were cast in order to establish the correct procedure for the stress freezing cycle and the slice cutting operation, and also to determine material fringe values precisely. The slicing and sub-slicing plan discussed was used and SCF at the point of interest were presented for boundary conditions. Experimental results were found to be very close to FEM results with a variation of 2-5 %. Hence, the experimental results were validated through finite element analysis.

4. Conclusions

Experimental work based on the circular polariscope was carried out by three dimensional photoelastic approach. The present work was performed for a square plate with a hole under transverse loading for simply supported boundary conditions. The experimental results were also compared with FEM results. The calculation of maximum stresses was done by procurement of fringe order near the discontinuities in the form of slices and sub-slices. The photoelastic results and FEM results varied between -2.66 to 4.44%. The accurate evaluation of stress state and SCF for three dimensional problems is a complex task, and was performed carefully in the present work. The experimental results are in substantial agreement with the FEM results.

Table 4. Fringe patterns for slices of samples 3 and 4 with hole diameter 0.02 m.

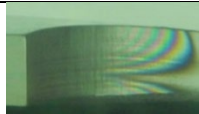
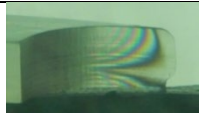
Light	Slice No.	Z-Direction	X-Direction	Zoomed View	Fringe Direction and Counting
White	3.1				 1.5 0.5
	3.2				
	4.1				
	4.2				
Monochromatic	3.1				1.5 0.5
	3.2				
	4.1				
	4.2				

Table 5. Fringe patterns for slices of samples 5 and 6 with hole diameter 0.02 m

Light	Slice No.	Z-Direction	X-Direction	Zoomed View	Fringe Direction and Counting
White	5.1				↑
	5.2				
	6.1				
	6.2				
Monochromatic	5.1				
	5.2				
	6.1				
	6.2				

Table 6. Fringe patterns for slices and sub-slices of samples 7 and 8 in solid plate

Light	Slice No.	Z-Direction	X-Direction	Fringe Direction and Counting
White	7.2			0.5
	7.3			
	8.2			
	8.2			
Monochromatic	7.2			→ 0.5
	7.3			→ 0.5
	8.2			→ 0.5
	8.2			→ 0.5

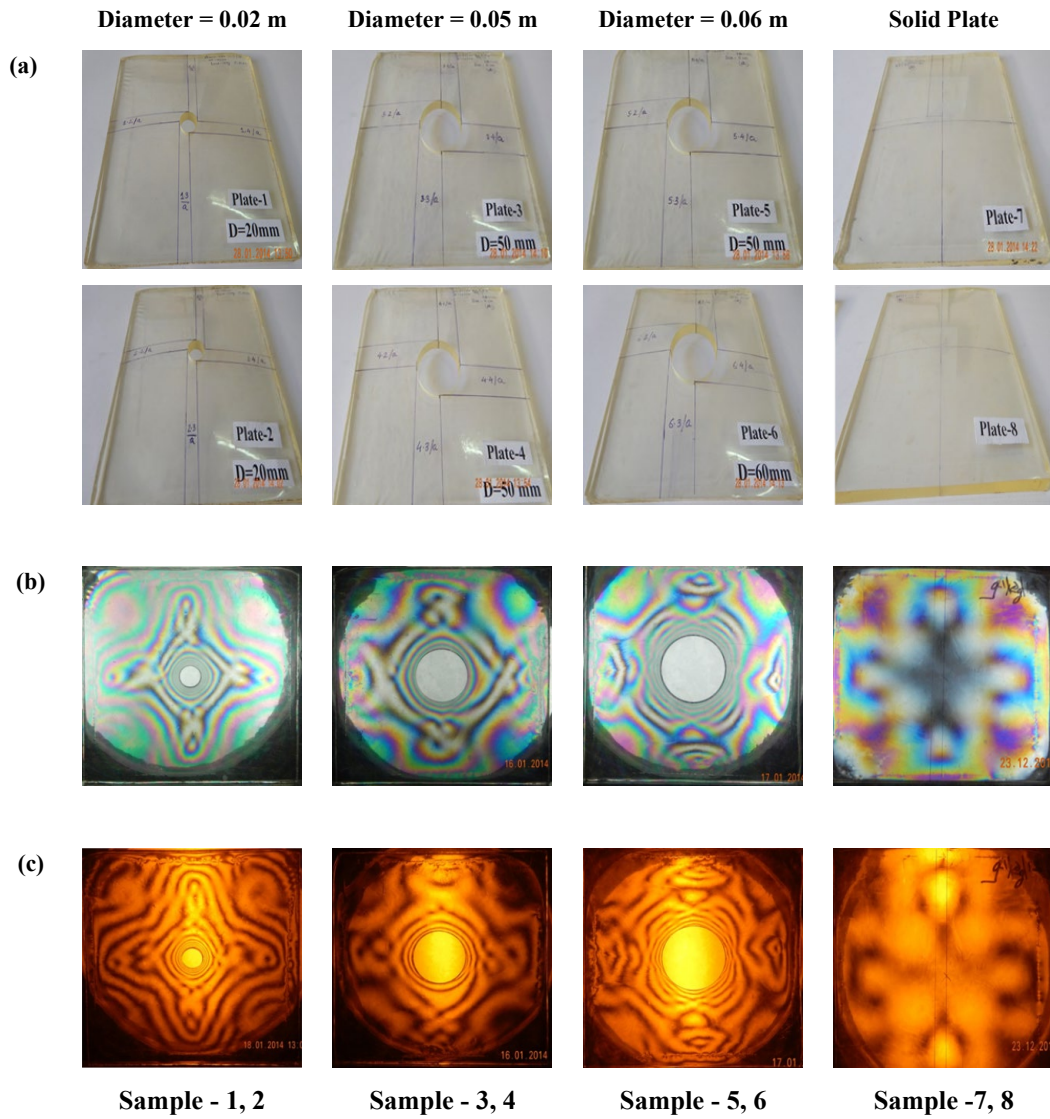


Figure 12. (a) Stress frozen plates (b) isochromatic fringes under white and monochromatic light

Table 7. SCF evaluation from experimental and numerical studies

Sample No.	Diameter of Hole (m)	Circular Disc Specimen		Slice No.	N	h _y (m)	σ _ξ (N/μ ²)	SCF		% Error
		No.	f _σ					Experimental	FEM	
Plate models with hole										
1	0.02	1	111.0	1.1-1.3	2.0	0.002	115643.7	1.92	1.84	.34
2				2.1-2.3						
3	0.05	2	147.9	3.1-3.3	1.5	0.002	87893.7	1.46	1.50	-2.66
4				4.1-4.3						
5	0.06	3	121.0	5.1-5.2	2.0	0.003	85310.4	1.41	1.35	4.44
6				6.1-6.2						
Solid Plate										
7	Solid plate	4	111.0	7.1-7.3	0.5	h _{y1}	60143.78			
8				8.1-8.4		0.001				

5. Acknowledgements

Authors acknowledge the authorities of N.I.T, Raipur for permitting the above work to be carried out in the Department of Mechanical Engineering.

References

- [1] Ramakrishnan, V. and Ramesh K., 2017. Scanning schemes in white light photoelasticity. Part II: Novel fringe resolution guided scanning scheme. *Optical Lasers Engineering*, 92, 141-149.
- [2] Ramesh, K. and Deshmukh, S.S., 1996. Three fringe photoelasticity-use of colour image processing hardware to automate ordering of isochromatics. *Strain*, 32(3), 79-86.
- [3] Patil, P., Vyasrayani, C.P. and Ramji, M., 2017. Linear least squares approach for evaluating crack tip fracture parameters using isochromatic and isoclinic data from digital photoelasticity. *Optical Lasers Engineering*, 93, 182-94.
- [4] Perumal, L., Tso, C.P. and Leng, L.T., 2016. Analysis of thin plates with holes by using exact geometrical representation within XFEM. *Journal of Advance Research*, 7, 445-452.
- [5] Ramesh, K. and Ramakrishnan, V., 2016. Digital photoelasticity of glass: A comprehensive review. *Optical Laser Engineering*, 87, 59-74.
- [6] Ajovalasit, A., Petrucci, G. and Scafidi, M., 2014. Review of RGB photoelasticity. *Optical Lasers Engineering*, 68, 58-73.
- [7] Swain, D., Thomas, B.P., Philip, J. and Pillai, S.A., 2014. Novel calibration and color adaptation schemes in three fringe RGB photoelasticity. *Optical Lasers Engineering*, 66, 320-329.
- [8] Shang, W., Ji, X. and Yang, X., 2015. Study on several problems of automatic full-field isoclinic parameter measurement by digital phase shifting photoelasticity. *Optik-International Journal of Light and Electron*, 126, 1981-1985.
- [9] Enab, T.A., 2014. Stress concentration analysis in functionally graded plates with elliptic holes under biaxial loadings. *Ain Shams Engineering Journal*, 5, 839-850.
- [10] Pandya, Y. and Parey, A., 2013. Experimental investigation of spur gear tooth mesh stiffness in the presence of crack using photoelasticity technique. *Engineering Failure Analysis Journal*, 34, 488-500.
- [11] Kale, S. and Ramesh, K., 2013. Advancing front scanning approach for three-fringe photoelasticity. *Optical Lasers Engineering*, 51, 592-599.
- [12] Forte, P., Paoli, A. and Razionale, A.V., 2013. A CAE approach for the stress analysis of gear models by 3D digital photoelasticity. *International Journal Interactive Design Manufacturing*, 9, 31-43.
- [13] Lee, Y.C., Liu, T.S., Wu, C.I. and Lin, W.Y., 2012. Investigation on residual stress and stress-optical coefficient for flexible electronics by photoelasticity. *Journal of International measurement confederation*, 45, 311-316.
- [14] Prasad, D.K., Ramana, K.V. and Rao, N.M., 2019. Theoretical investigation of stresses induced at blade mounting locations in steam turbine rotor system. *International Journal of Applied Mechanics and Engineering*, 24(2), 295-307.